



## OPEN ACCESS

## EDITED BY

Damien Paul Devos,  
Spanish National Research Council  
(CSIC), Spain

## REVIEWED BY

Arthur Charles-Orszag,  
University of California, San Francisco,  
United States

Burak Avci,  
Aarhus University, Denmark  
Alex Bisson,  
Brandeis University, United States

## \*CORRESPONDENCE

Iain G. Duggin  
✉ iain.duggin@uts.edu.au

RECEIVED 02 August 2024

ACCEPTED 28 October 2024

PUBLISHED 22 November 2024

## CITATION

Brown HJ and Duggin IG (2024) MinD proteins regulate CetZ1 localization in *Haloferax volcanii*. *Front. Microbiol.* 15:1474697. doi: 10.3389/fmicb.2024.1474697

## COPYRIGHT

© 2024 Brown and Duggin. This is an open-access article distributed under the terms of the [Creative Commons Attribution License \(CC BY\)](https://creativecommons.org/licenses/by/4.0/). The use, distribution or reproduction in other forums is permitted, provided the original author(s) and the copyright owner(s) are credited and that the original publication in this journal is cited, in accordance with accepted academic practice. No use, distribution or reproduction is permitted which does not comply with these terms.

# MinD proteins regulate CetZ1 localization in *Haloferax volcanii*

Hannah J. Brown and Iain G. Duggin\*

Australian Institute for Microbiology and Infection, University of Technology Sydney, Ultimo, NSW, Australia

CetZ proteins are archaea-specific homologs of the cytoskeletal proteins FtsZ and tubulin. In the pleomorphic archaeon *Haloferax volcanii*, CetZ1 contributes to the development of rod shape and motility, and has been implicated in the proper assembly and positioning of the archaellum and chemotaxis motility proteins. CetZ1 shows complex subcellular localization, including irregular midcell structures and filaments along the long axis of developing rods and patches at the cell poles of the motile rod cell type. The polar localizations of archaellum and chemotaxis proteins are also influenced by MinD4, the only previously characterized archaeal member of the MinD family of ATPases, which are better known for their roles in the positioning of the division ring in bacteria. Using *minD* mutant strains and CetZ1 subcellular localization studies, we show here that a second *minD* homolog, *minD2*, has a strong influence on motility and the localization of CetZ1. Knockout of the *minD2* gene altered the distribution of a fluorescent CetZ1-mTq2 fusion protein in a broad midcell zone and along the edges of rod cells, and inhibited the localization of CetZ1-mTq2 at the cell poles. MinD4 had a similar but weaker influence on motility and CetZ1-mTq2 localization. The *minD2/4* mutant strains formed rod cell shapes like the wildtype at an early log stage of growth. Our results are consistent with distinct roles for CetZ1 in rod shape formation and at the poles of mature rods, that are positioned through the action of the MinD proteins and contribute to the development of swimming motility in multiple ways. They represent the first report of MinD proteins controlling the positioning of tubulin superfamily proteins in archaea.

## KEYWORDS

cytoskeleton, motility, protein localization, tubulin superfamily, halophile, archaea

## Introduction

Spatial and temporal regulation of protein subcellular localization is critical for the proper function of all cells. In bacteria, there are several different classes of proteins from the ParA/MinD superfamily (Leipe et al., 2002), which coordinate positioning of flagella (Schuhmacher et al., 2015a,b), chemosensory arrays (Ringgaard et al., 2011; Roberts et al., 2012), chromosomes (Jalal and Le, 2020), plasmids (Baxter and Funnell, 2015), cell division cytoskeletal proteins (Lutkenhaus, 2007; Hu and Lutkenhaus, 2001), and various other molecules or structures (Lutkenhaus, 2012; Perez-Cheeks et al., 2012; Laloux and Jacobs-Wagner, 2014; Thompson et al., 2006; Savage et al., 2010). A key characteristic of ParA/MinD superfamily proteins is their ATPase activity (Loose et al., 2011; Howard and Kruse, 2005) and dimerization (Hu and Lutkenhaus, 2001; Dunham et al., 2009) involving amino acid residues within a deviant Walker A motif (Leipe et al., 2002; Lutkenhaus, 2012). In MinD proteins, a subset of proteins within the ParA/MinD superfamily, this ATP binding and hydrolysis drives intracellular Min system dynamics that can generate concentration gradients of Min proteins

(Baxter and Funnell, 2015; Loose et al., 2011; Howard and Kruse, 2005). In bacteria, these gradients are critical for the correct positioning of FtsZ, a key cell division protein and tubulin superfamily homolog (Bi et al., 1991; Erickson, 1995; Nogales et al., 1998), at mid-cell to help ensure symmetric division of the mother cell into two daughter cells (Hu and Lutkenhaus, 2001; Raskin and De Boer, 1999; De Boer et al., 1989).

The Min system of *Escherichia coli* is the prototypical example of Min system dynamics and function in bacteria. MinD oscillates between poles of the rod-shaped cells, controlled by its regulator MinE, and carries MinC an FtsZ antagonist. Together, these proteins generate dynamic concentration gradients of MinCD which is on average highest at cell poles and lowest at mid-cell, preventing Z-ring formation anywhere other than at mid-cell (Lutkenhaus, 2007). MinE accelerates the ATPase activity of MinD (Loose et al., 2011) and drives its release from the membrane which it is bound to via a membrane targeting sequence (Lackner et al., 2003; Park et al., 2011; Szeto et al., 2002). Together these proteins constitute a reaction-diffusion system driven by the hydrolysis of ATP. Disruption of MinD ATPase activity blocks oscillation and function completely (Zhou et al., 2005; Lutkenhaus and Sundaramoorthy, 2003).

ParA/MinD family homologs have been identified across the archaeal domain, but MinD homologs are particularly abundant in *Euryarchaea* (Nußbaum et al., 2020). In the model halophilic archaeon, *Haloferax volcanii*, there are four MinD paralogs. The functions of MinD1-3 (HVO\_0225, HVO\_0595, and HVO\_1634, respectively) have not been described and no clear protein partners equivalent to bacterial MinE have been identified. MinD4 (HVO\_0322) has been characterized and is known to oscillate between cell poles, as well as concentrating with a cap-like appearance at the poles (Nußbaum et al., 2020). Surprisingly, the oscillation was not dependent on the ATPase Walker A or Walker B motifs, but the cap-like structures were, suggesting that the oscillation is driven by an alternative energy source (Nußbaum et al., 2020). Furthermore, although *H. volcanii* possess FtsZ homologs, none of the MinD paralogs were found to have a role in the mid-cell positioning of FtsZ; simultaneous deletion of all four paralogs had no detected effect on FtsZ positioning. Instead, deletion of *minD4* caused a motility defect and reduced the polar positioning of key protein constituents of the archaeum and chemotaxis arrays, ArlD and CheW, respectively (Nußbaum et al., 2020). Furthermore, disruption of MinD4 predicted ATPase activity through mutations to the Walker A or Walker B motifs, or truncation of its extended C-terminal tail all result in motility defects. Potential roles of the other MinD paralogs in motility of *H. volcanii* have not been reported.

Although the archaeum and chemosensory arrays are considered the core motility machinery in *H. volcanii*, there are many other contributing factors, and a range of proteins with a variety of primary functions have been shown to influence motility (Tripepi et al., 2010, 2012; Abdul Halim et al., 2013, 2020; Esquivel and Pohlschroder, 2014; Cerletti et al., 2014; Chatterjee et al., 2024; Hackley et al., 2024; Duggin et al., 2015; Schiller et al., 2024). CetZ cytoskeletal proteins, a group of tubulin superfamily proteins specific to archaea and abundant in Haloarchaea (Duggin et al., 2015; Aylett and Duggin, 2017; Brown and Duggin, 2023),

have been implicated in the control of cell shape and motility (Duggin et al., 2015; de Silva et al., 2024). The most well-studied and highly conserved CetZ homolog, CetZ1, is necessary for rod-shape development and swimming motility (Duggin et al., 2015; de Silva et al., 2024). Our recent results have suggested that CetZ1 is an important factor for the proper assembly and positioning of motility proteins ArlD and CheW (Brown et al., 2024). It is not yet clear whether CetZ1 contributes to motility solely via its essential role in rod shape development (Duggin et al., 2015), or whether it has other functions that promote motility. It also is not yet clear how MinD4 and CetZ1 might coordinate their activities to regulate positioning and assembly of motility machinery.

Currently, no connection between Min proteins and FtsZ or other tubulin superfamily homologs, such as the CetZs, has been reported in archaea. Here, we investigate the potential for MinD homologs of *H. volcanii* to control positioning of CetZ1 and identify MinD2 as a strong regulator of CetZ1 localization in rod cells. This is consistent with a model in which a hierarchy or network of proteins is involved in promoting the development of motility structures at the cell poles.

## Methods

### Growth and culturing

*Haloferax volcanii* was routinely grown in Hv-Cab (de Silva et al., 2021) medium supplemented with uracil (50 µg/ml) to fulfill auxotrophic requirements if necessary, or L-Tryptophan (1 mM) to induce expression of genes under the control of the *p.tna* promoter. Liquid cultures were grown at 42°C with shaking (200 rpm).

### Strain and plasmid construction

Strains, plasmids and oligonucleotides used in this study are listed in Supplementary Tables S1–S3, respectively. *H. volcanii* H26 ( $\Delta pyrE2$   $\Delta pHV2$ ) was used as the wildtype parent strain for construction of mutant strains. All strains investigated in experiments contained a pHV2-based vector (pTA962 vector or derivatives) to complement the *pyrE2* auxotrophic marker and better match the original *H. volcanii* wild-type genotype; previous work has shown that the base strains with  $\Delta pyrE2$ ,  $\Delta hdrB$  or  $\Delta pHV2$  show poorer expression of the cell morphology and motility phenotypes, which are sensitive to nutrient and culture conditions (Duggin et al., 2015; de Silva et al., 2021; Patro et al., 2023).

To create chromosomal point mutations in *minD2*, generating strains ID810 (*minD2WA*\*) and ID811 (*minD2WB*\*), H26 was transformed with vectors pTA131\_minD2WA or pTA131\_minD2WB, respectively, using previously described transformation methods (Cline et al., 1989) and the homologous recombination-based “pop-in pop-out” method (Allers et al., 2004) was used to replace the native *minD2* gene with Walker A (K16A, AAG to GCC) or Walker B (D117A, GAT to GCC) mutant alleles. Primers MinD2\_USflank\_extF (forward) and MinD2\_DSflank\_extR (reverse), designed to bind externally to the

regions of homologous recombination, were then used to amplify the *minD2* locus. The resultant PCR products were purified, and then sequenced by Sanger sequencing (Australian Genome Research Facility) to identify transformants carrying the expected mutations. All strains using *minD2WA\** (ID810) as the parent strain were also verified by checking for complete conversion of alleles and the absence of potential suppressor mutations (SNPs, indels) using Illumina whole-genome sequencing with ~50X coverage.

Plasmids for the expression of *minD2*, *minD2WA\**, and *minD2WB\** were generated by amplifying these open reading frames from *H. volcanii* H26 (ID621), ID810, and ID811, respectively. Forward and reverse primers for this reaction incorporated NdeI and BamHI restriction sites at 5' and 3' ends, respectively. ORFs were then ligated between the same restriction sites in pTA962 (Allers et al., 2010), generating pHJB63-65 which were sequence verified.

pHJB72 for the dual expression of *cetZ1-G-mTq2* and *minD2* was generated by amplifying the *minD2* open reading frame from pHJB63, incorporating an XbaI site at the 5' end. The amplicon was then ligated between NheI and NotI of pHVID135. Plasmids and oligonucleotides used in this study are listed in [Supplementary Tables S2, S3](#), respectively.

## Soft-agar motility assays

Soft-agar motility assays were carried out as described in [Brown et al. \(2024\)](#), using Hv-Cab with 0.25% (w/v) agar and 1 mM L-Tryptophan. Motility was quantified by averaging perpendicular measurements of the motility halo diameter after 3 days of incubation of the plates inside a plastic bag at 42°C.

## Light microscopy

To prepare samples for microscopy, single colonies were first used to inoculate 3 ml Hv-Cab medium, each representing a single culture (biological) replicate. These cultures were allowed to grow to OD<sub>600</sub> ~0.6. Then, 3 µl of this culture was taken to inoculate 10 ml Hv-Cab supplemented with 1 mM L-Tryptophan and grown for 18 h (OD<sub>600</sub> ~0.1). A 2 µl droplet of cells was spotted onto a 1.5% agarose pad containing 18% BSW as described in [Duggin et al. \(2015\)](#). Samples were then covered with a clean #1.5 glass coverslip.

Imaging for phase-contrast and fluorescence microscopy was carried out using a V3 DeltaVision Elite (GE Healthcare) with an Olympus UPLSAPO 100X NA 1.4 objective and pco.edge 5.5 sCMOS camera. A filter set for mTurquoise2/CFP (excitation = 400–453, emission = 463–487) was used for imaging of CetZ1-mTq2 expressing strains. 3D Structured-illumination microscopy (3D-SIM) was conducted as described previously ([de Silva et al., 2024](#)) using a DeltaVision OMX SR microscope (GE Healthcare) and a DAPI filter for excitation (405 nm) and an AF488 filter for emission (504–552 nm), suitable for imaging of mTurquoise2. Raw images were reconstructed using SoftWorx (Applied Precision, GE Healthcare), and 3D

renders were generated ([Schmid et al., 2019](#)) using Bitplane IMARIS (v9.6.0).

## Image analysis

Image analysis was conducted using the MicrobeJ (v5.131) ([Ducret et al., 2016](#)) plugin for FIJI (v2.14.0/1.54f) ([Schindelin et al., 2012](#)). Cell shape characteristics were analyzed using phase-contrast images and default settings. Fluorescent foci detection was carried out after background subtraction with a ball size of 50 pixels, and the *point* detection method was used for analysis of CetZ1-mTq2 localization (Tolerance = 200).

Fluorescence intensity profiles along the long axis of each cell were generated using the *XStatProfile* function in MicrobeJ (the long axis was normalized between 0 and 1). The mean and standard deviation of the raw fluorescence intensity over all cells were then determined (Stat = mean ± stdv, Y-axis = MEDIAL.intensity.ch2, number of bins = 50). The intensity data were also normalized (0–100%) and the median fluorescence intensity along the long axis determined for each culture replicate (Stat = median, Y-axis = MEDIAL.intensity.ch2, number of bins = 50), and then the mean and standard error of all culture replicates were plotted. These data were also displayed as the difference in fluorescence intensity between *minD* deletion or Walker mutant backgrounds and the wildtype background.

Heatmaps of foci localization were generated using pooled data from all culture replicates and the *XYCellDensity* function (Rendering = Density) with default settings.

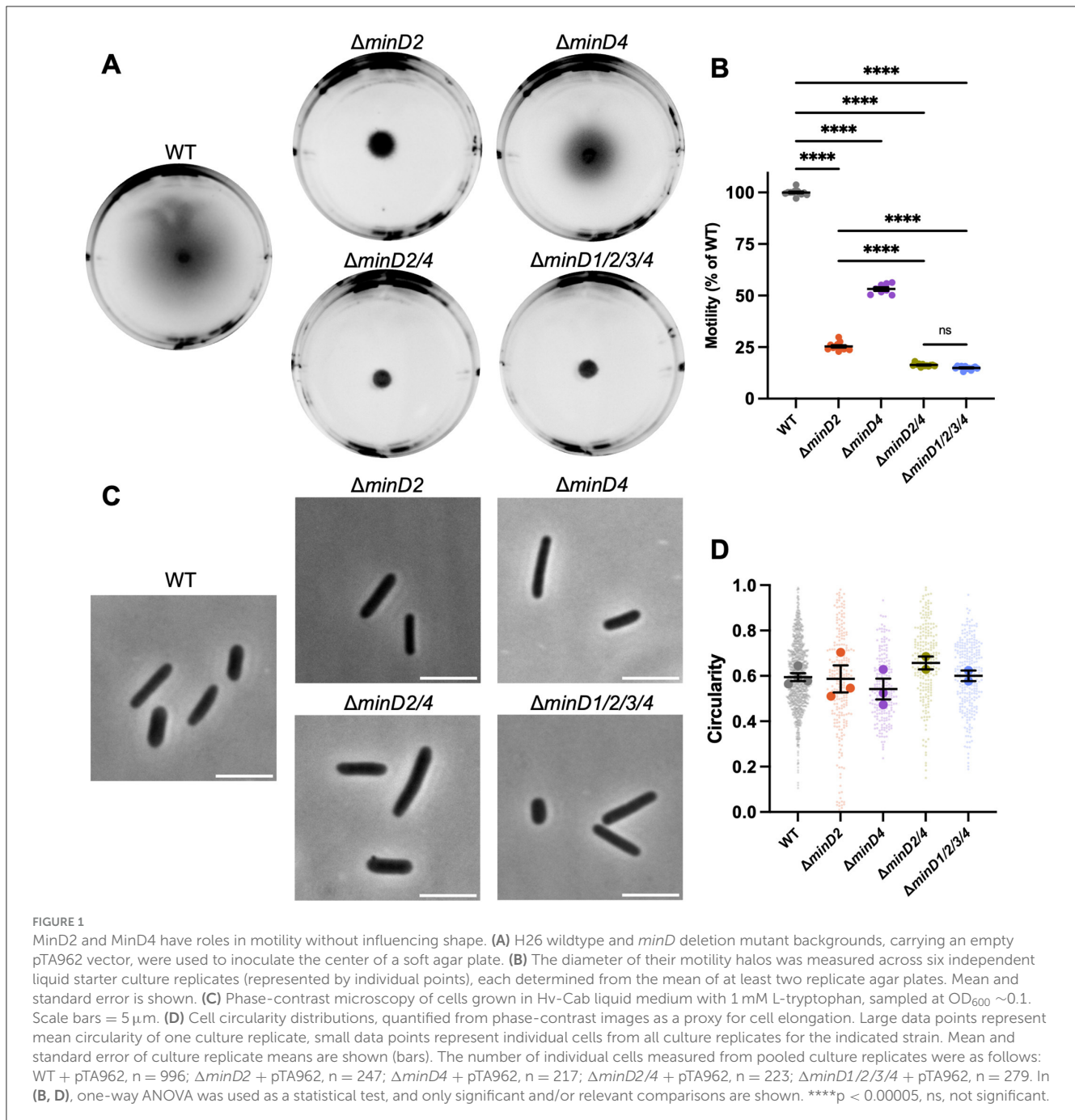
## Results

### Deletion of *minD2* or *minD4* results in motility defects with normal rod cell shape

We began by assessing the effect of *H. volcanii minD* gene deletions on motility, focussing on MinD2 and MinD4, which are expressed significantly in standard culture conditions ([Babski et al., 2016](#); [Cerletti et al., 2018](#); [Laass et al., 2019](#)). MinD4 has previously been studied in this context ([Nußbaum et al., 2020](#)). The *minD* deletion strains grew at rates like the wildtype in starter cultures, and motility was assessed using soft-agar motility assays in which cells develop into a motile rod form ([Duggin et al., 2015](#)) and then swim out through the gel from a central inoculation point, forming a halo.

Deletion of *minD2* resulted in a motility defect (~25% of the halo diameter compared to wildtype), which was significantly stronger than that caused by deletion of *minD4* (~50% of wildtype motility; [Figures 1A, B](#)). Deletion of both *minD2* and *minD4* resulted in a stronger motility defect (~16% of wildtype motility). The deletion of all four *minD* homologs ( $\Delta minD1/2/3/4$ ) was indistinguishable to that of the  $\Delta minD2/4$ .

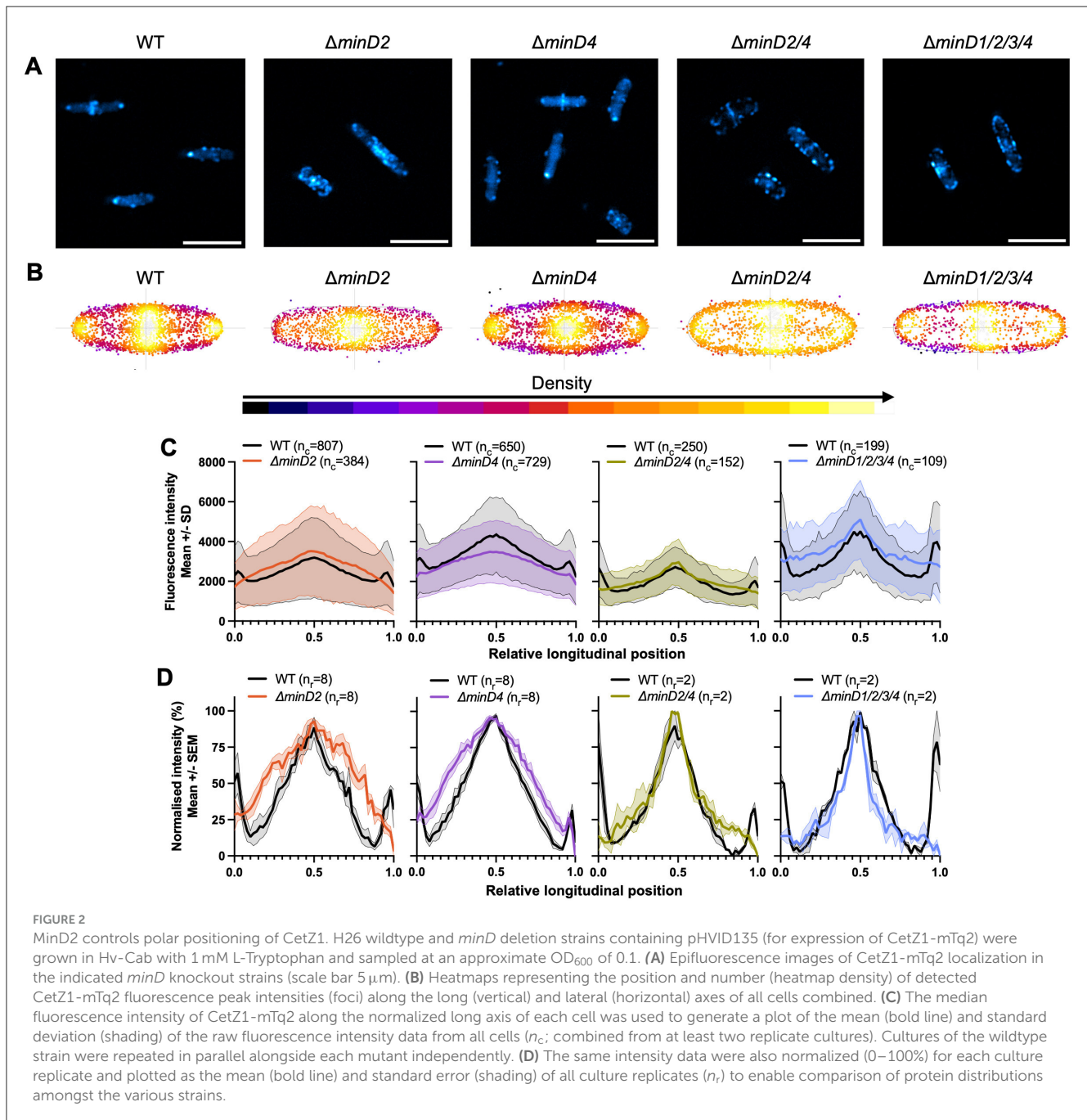
*H. volcanii* is pleomorphic and cultures can show a range of cell shapes including irregular disk, or plate-shaped cells, and rods with varying widths and degrees of elongation ([Duggin et al., 2015](#);



de Silva et al., 2021). Furthermore, a motile-rod cell type with regular cell widths develops under certain conditions to promote swimming (Duggin et al., 2015; Li et al., 2019). To determine whether the two MinD proteins are required for rod formation, which might contribute to their effects on motility, we sampled wild-type and  $\Delta minD2/4$  cells from the early-log phase of liquid batch cultures (OD ~0.1), where motile rods are prevalent (de Silva et al., 2021; Li et al., 2019). By quantifying cell circularity as an indicator of the extent of cell elongation, we observed no significant cell shape differences at this stage of growth in any of the strains (Figures 1C, D).

## MinD2 and MinD4 influence the cellular positioning of CetZ1

MinD4 has been shown to have a role in the polar positioning of the archaellum and chemotaxis arrays through the use of tagged marker proteins ArlD and CheW, respectively (Nußbaum et al., 2020). We recently found that CetZ1 also influences the proper assembly and positioning of ArlD and CheW (Brown et al., 2024). It is unknown whether MinD4 and CetZ1 cooperate or work independently to promote motility. To begin investigating this, we sought to determine whether



the absence of MinD2 or MinD4 affects the localization of CetZ1.

To do this, we observed the localization of a CetZ1-mTurquoise2 (mTq2) fusion protein (Ithurbide et al., 2024) in the wildtype and various *minD* deletion strain backgrounds. Fluorescence microscopy of CetZ1-mTq2 in wildtype cells imaged in early-log growth (OD<sub>600</sub> ~0.1; Figure 2A), showed the expected patchy localization with relatively high fluorescence at cell poles and the mid-cell region (de Silva et al., 2024; Brown et al., 2024; Ithurbide et al., 2024). To characterize these patterns, we analyzed the whole population of cells, in the wildtype and *minD* mutant backgrounds, by generating heatmaps that represent the position and frequency of fluorescent foci within a normalized cell shape

(reflecting the averaged aspect ratio; Figure 2B). We also generated plots of the total and normalized mean fluorescence intensity of CetZ1-mTq2 along the long-axis of the cells (Figures 2C, D). In the  $\Delta minD2$  background, CetZ1-mTq2 localization remained patchy and concentrated in a broad zone near midcell, which was noticeably broader compared to the wildtype, and the high-intensity polar localisations of CetZ1-mTq2 were not observed (e.g., Figures 2A, C, D). These patterns were also reflected in the number of fluorescent foci detected along the cell lengths (Figure 2B); the wildtype background displayed clear peaks of fluorescence around midcell and at the cell poles, but in the  $\Delta minD2$  background the midcell foci were more spread out along the cell length, and showed almost complete loss of the polar clusters of foci.

To confirm whether the changes to CetZ1-mTq2 localization patterns were resultant from the loss of *minD2* specifically, we observed CetZ1-mTq2 localization when *minD2* deletion was complemented by expression of *minD2* from a plasmid containing the open reading frames for *cetZ1-mTq2* and *minD2* in tandem, under the control of the inducible *p.tna* promoter (Supplementary Figure S1). Dual expression of these genes in the  $\Delta minD2$  background using 1 mM L-Tryptophan did not clearly restore the CetZ1-mTq2 localization defect (Supplementary Figures S1a, b). However, when 2 mM L-Tryptophan was used, the localization of CetZ1-mTq2 was partially restored (Supplementary Figures S1c–g), confirming that *minD2* regulates the localization of CetZ1. The requirement for the additional tryptophan to observe partial complementation is likely due to a sensitivity of the phenotype to the expression level of *minD2*, which is likely to be influenced by its second position in the tandem expression plasmid (Ithurbide et al., 2024).

A weaker defect of CetZ1-mTq2 polar localization was also observed in the  $\Delta minD4$  background (compare the polar intensities between mutant and wildtype in Figure 2D). Additional control experiments demonstrated that the  $\Delta minD$  strains producing CetZ1-mTq2 had no significant differences in shape compared to the wildtype control (OD  $\sim$ 0.1), and we also observed an equivalent motility defect with or without the CetZ1-mTq2 fusion (Supplementary Figures S2a, b). The results in Figure 2 also revealed that the zone of CetZ1-mTq2 localization around the midcell region was broadened in the absence of either MinD2 or MinD4 (Figures 2B, D). Interestingly, such broadening was not apparent in strains in which both *minD2* and *minD4* were deleted, although the polar localization of CetZ1-mTq2 was still strongly inhibited (Figures 2B, D). This suggests that the midcell zone of CetZ1-mTq2 localization is impacted when only one of MinD2 or MinD4 is present and implies a genetic interaction or interference between *minD2* and *minD4* that influences midcell CetZ1.

## Structural characteristics of CetZ1-mTq2 localization in individual cells lacking *minD2* or *minD4*

We further resolved structural characteristics of the CetZ1-mTq2 polar localizations and the effects of the *minD* knock-outs, using three-dimensional structured-illumination microscopy (3D-SIM). Multiple cells are shown as maximum intensity projections in Figures 3A–C to visualize the effect of the mutations on CetZ1 structures in individual cells and facilitate comparisons to the aggregate data shown in Figures 2B–D.

In wildtype early-log cells, CetZ1-mTq2 often appeared as a bright focus, doublet, multi-lobed, or cap-like structure at the cell poles, suggestive of a ring or disc-like structure at the tip of the cell pole (Figures 3A, D). Patches and filaments were also observed along the cell edges in the midcell zone. In the absence of MinD2, the foci of CetZ1-mTq2 appeared more randomly distributed around the cells, with no clear preference for the cell poles or the midcell zone (Figure 3B). In the absence of MinD4, this effect was weaker, and some of the cells still appeared to show the relatively bright polar tip structures of

CetZ1-mTq2 (Figure 3C). The  $\Delta minD2$  and  $\Delta minD4$  backgrounds also showed noticeably more of the CetZ1-mTq2 patches or foci throughout the cell area compared to the wildtype (Figures 3A–C). By inspecting the slice series of images to resolve the 3D detail (Figure 3E, Supplementary Video 1), CetZ1-mTq2 foci appeared noticeably more prevalent at the top and bottom surfaces along the length of the *minD* mutant cells, compared to the wildtype, and potentially in the cytoplasm too (Supplementary Videos 2–4). These observations are consistent with the broadening of the midcell zone and reduced polar positioning of CetZ1-mTq2 in the *minD* mutants seen in the aggregated epifluorescence data (Figures 2B–D).

## ATPase active-site residues of MinD2 are required for normal swimming motility and polar localization of CetZ1

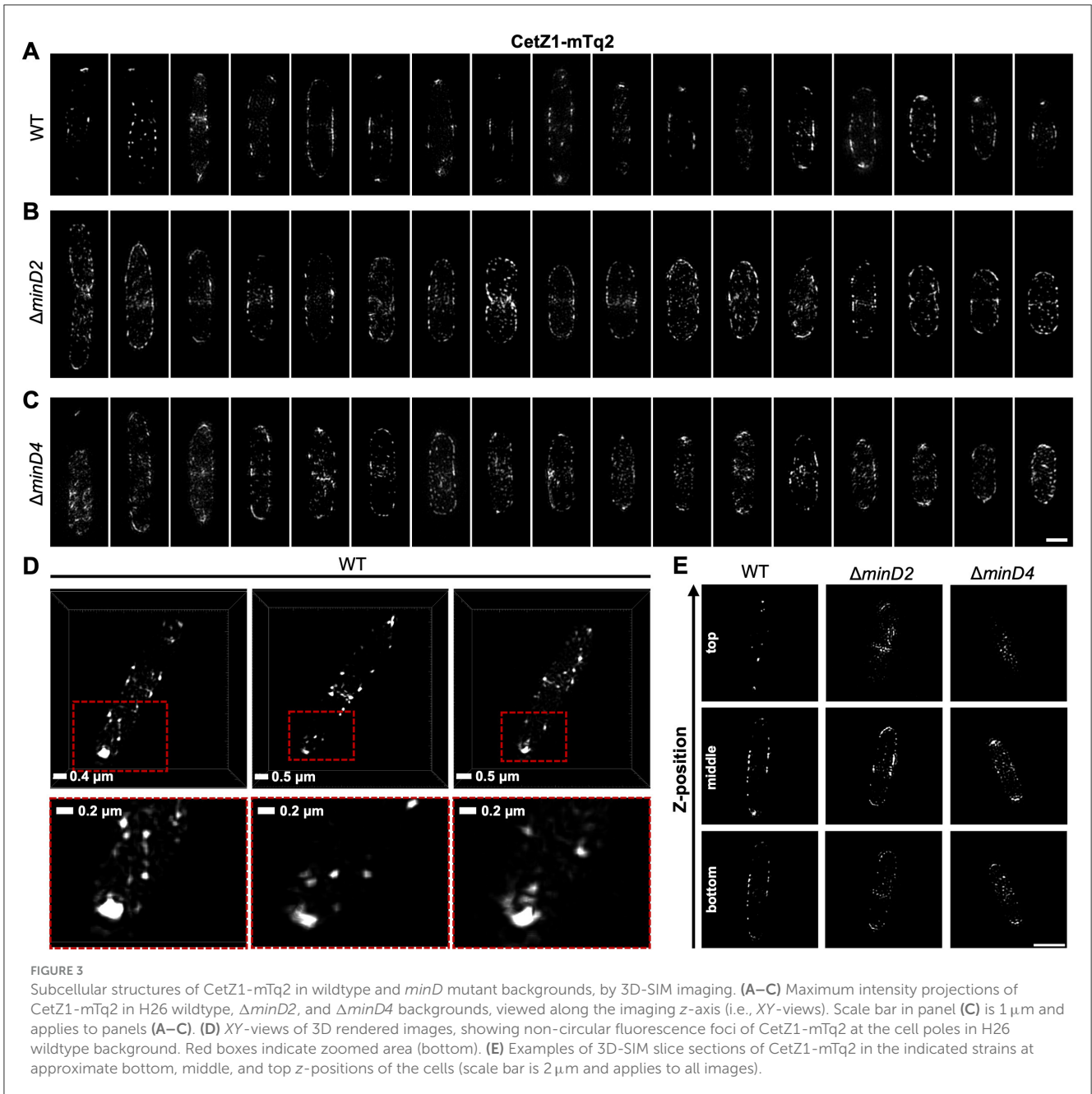
MinD proteins typically rely on ATP hydrolysis to drive their dynamic localization patterns, such as oscillation between cell poles, generating concentration gradients which form the basis for their spatial and temporal control of downstream proteins (Lutkenhaus, 2012; Lutkenhaus and Sundaramoorthy, 2003; Nußbaum et al., 2020). When the Walker A and Walker B motifs of *H. volcanii* MinD4 were previously mutated to disrupt ATP binding and hydrolysis, swimming motility was reduced and polar localization of MinD4 was disrupted, although not its oscillation (Nußbaum et al., 2020).

Given that MinD2 had the strongest effects on swimming motility and CetZ1 localization, we chose to further investigate the importance of the ATPase active-site for MinD2 functionality in motility and CetZ1 localization. We generated chromosomal point-mutations in the endogenous *minD2* gene in the ATPase active site via the deviant Walker A (K16A) and Walker B (D117A) motifs, here forth referred to as *minD2WA\** and *minD2WB\**, respectively. These mutations are equivalent to those previously made in *minD4* (Nußbaum et al., 2020).

Both *minD2WA\** and *minD2WB\** strains (containing the empty vector pTA962) partially perturbed motility, resulting in  $\sim$ 78 and  $\sim$ 36% of the wildtype motility halo diameter, respectively (Figures 4A, C), compared to the complete deletion of *minD2* ( $\sim$ 25%, Figures 1A, B). The motility defect of  $\Delta minD2$  was complemented by expressing *minD2* from a plasmid (pTA962 backbone), confirming the important role of *minD2* in motility (Figures 4B, C).

When *minD2WA\** was expressed from a plasmid in the  $\Delta minD2$  background, this strain had a more pronounced motility defect ( $\sim$ 35%) compared to the chromosomal mutant *minD2WA\** ( $\sim$ 78%). This might be related to different expression levels of *minD2WA\** in the plasmid with *p.tna* compared to its native chromosomal site. Expression of *minD2WB\** from pTA962 in  $\Delta minD2$  produced equivalent motility to the complete *minD2* deletion, consistent with its much stronger effects on motility observed with the chromosomal *minD2WB\** mutant (Figures 4B, C).

Phase-contrast microscopy and analysis of cell shape (circularity) confirmed that, like  $\Delta minD2$ , the *minD2WA\**



and *minD2WB\** mutations did not significantly affect rod shape (at OD  $\sim$ 0.1), whether expressed chromosomally (Supplementary Figures S3a, c) or from the plasmid (Supplementary Figures S3b, d).

We then assessed the effect of the *minD2WA\** and *minD2WB\** chromosomal mutants on CetZ1-mTq2 localization. Control experiments showed that expression of CetZ1-mTq2 did not impact cell circularity or motility of either the *minD2WA\** or *minD2WB\** strains (Supplementary Figures S3c, e). Fluorescence microscopy (Figure 5A) showed that both Walker mutations resulted in a substantial loss of CetZ1-mTq2 fluorescence intensity (Figure 5C) and foci localization at cell poles and showed the midcell zone broadening (Figure 5B) like in the  $\Delta minD2$  background (Figure 2).

## Discussion

MinD proteins and related protein families are important for spatial and temporal positioning of a variety of molecules but have mainly been characterized in bacteria (Lutkenhaus, 2012). One of four MinD paralogs in the archaeal model organism *H. volcanii*, MinD4, has previously been described to affect motility via regulating the positioning of archaellum and chemotaxis arrays, via unknown mechanisms (Nußbaum et al., 2020). The tubulin-like cytoskeletal protein CetZ1 is another factor promoting the proper assembly and positioning of these proteins at the cell poles (Brown et al., 2024). CetZ1 is needed for rod cell shape formation (Duggin et al., 2015), which may contribute to motility in several ways, and shows complex subcellular localization along the cell body and then

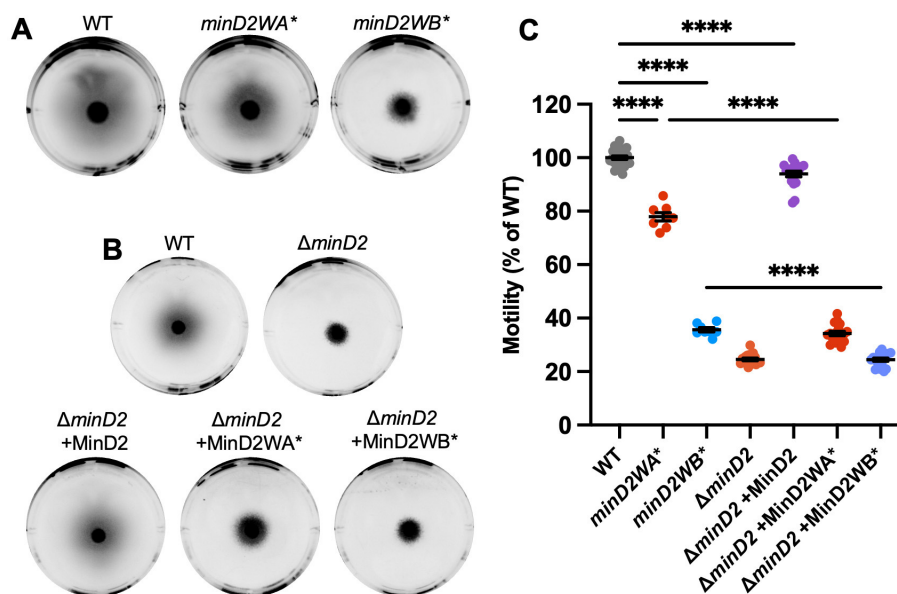


FIGURE 4

Chromosomal Walker mutants of *minD2* perturb motility. (A) H26 wildtype, *minD2WA\**, and *minD2WB\** backgrounds containing pTA962, (B) and  $\Delta$ *minD2* containing pTA962 were compared to  $\Delta$ *minD2* containing pHJB63-65 for expression of *minD2*, *minD2WA\**, and *minD2WB\**, respectively, and inoculated onto Hv-Cab soft agar (0.25 % w/v) supplemented with 1 mM L-Tryptophan. (C) Halo diameters were quantified across four starter culture replicates with two technical replicates (motility agar plates) each (indicated by individual points). Mean and standard error are shown. One-way ANOVA was used as a statistical test, and only significant and relevant comparisons are shown. \*\*\*\* $p < 0.00005$ .

at the cell poles of motile rods, where it is hypothesized to form a scaffold-like structure, though its mechanism of action at these sites is unclear.

We found here that MinD2 is important for motility and for the subcellular positioning of CetZ1. The potential relationship between these two functions is yet to be elucidated. Deletion of *minD2* was found to have a more severe motility defect than deletion of *minD4*, and deletion of both genes resulted in an even greater motility defect, suggesting distinct roles or additive contributions of these two MinD paralogs in motility. MinD2 and to a lesser extent MinD4 also influenced the subcellular positioning of CetZ1 in the midcell region and at the poles, in a manner that was independent of cell shape. CetZ1 has been implicated in distinct roles in establishing rod-shape during motile cell differentiation, and then at the poles of the mature motile rods (Duggin et al., 2015; Brown et al., 2024). Our results suggest that the effects of MinD2 on CetZ1 localization do not have an essential role in maintaining rod shape, because  $\Delta$ *minD2* cells could still form normal shaped rods at an early-mid log stage of culture.

We found that mutations in the Walker A and B motifs of the MinD2 ATPase both strongly influenced CetZ1 positioning along the cell length and poles, like the *minD2* deletion. However, only the Walker B mutant (D117A) strongly perturbed motility, whereas the Walker A (K16A) mutant (in its chromosomal context) resulted in only a mild motility defect. This suggests that MinD2 has an impact on motility that is largely independent of the K16 residue and CetZ1 positioning. The K16 residue is expected to be involved in nucleotide dependent dimerization (Lutkenhaus and Sundaramoorthy, 2003), so this function may not be critical to the overall motility function of MinD2, and instead plays

a role in CetZ1 positioning for an as yet unresolved purpose. Notably, the equivalent MinD4 Walker A and B mutants reduced motility equivalently to *minD4* deletion (Nußbaum et al., 2020). The MinD2 and MinD4 proteins could therefore have multiple, differing functions that contribute to the proper development of motile *H. volcanii* cells.

The accompanying study by Patro et al. (2024) found that MinD2 is required for normal motility and the proper polar localization of the archaellum and chemotaxis proteins, ArlD and CheW, like previously seen with MinD4 (Nußbaum et al., 2020). They also reported a difference in cell shape during the development of rod cells in the  $\Delta$ *minD2* compared to the wildtype. This likely represents an earlier phase of *H. volcanii* cultures, where cells are actively shapeshifting into motile rods (de Silva et al., 2021; Li et al., 2019), compared to the current study where rods had already formed, and we found that their cell shapes in the wildtype and  $\Delta$ *minD2* strains were indistinguishable. Though we note that since *H. volcanii* morphogenesis is highly sensitive to exact media composition and culture conditions (de Silva et al., 2021; Patro et al., 2023), excessive comparisons of the exact magnitudes or timing of events from separate studies should be avoided. Nevertheless, if the rate or timing of rod formation is influenced by MinD2 (Patro et al., 2024), this may affect another developmental stage of motility, such as the placement of Arl/Che proteins at the poles. However, it is still unclear whether any effects on cell shape development directly contribute to the *minD2*-dependent reduction of motility.

Considering the main findings from this and other recent studies (Nußbaum et al., 2020; Patro et al., 2024), we can

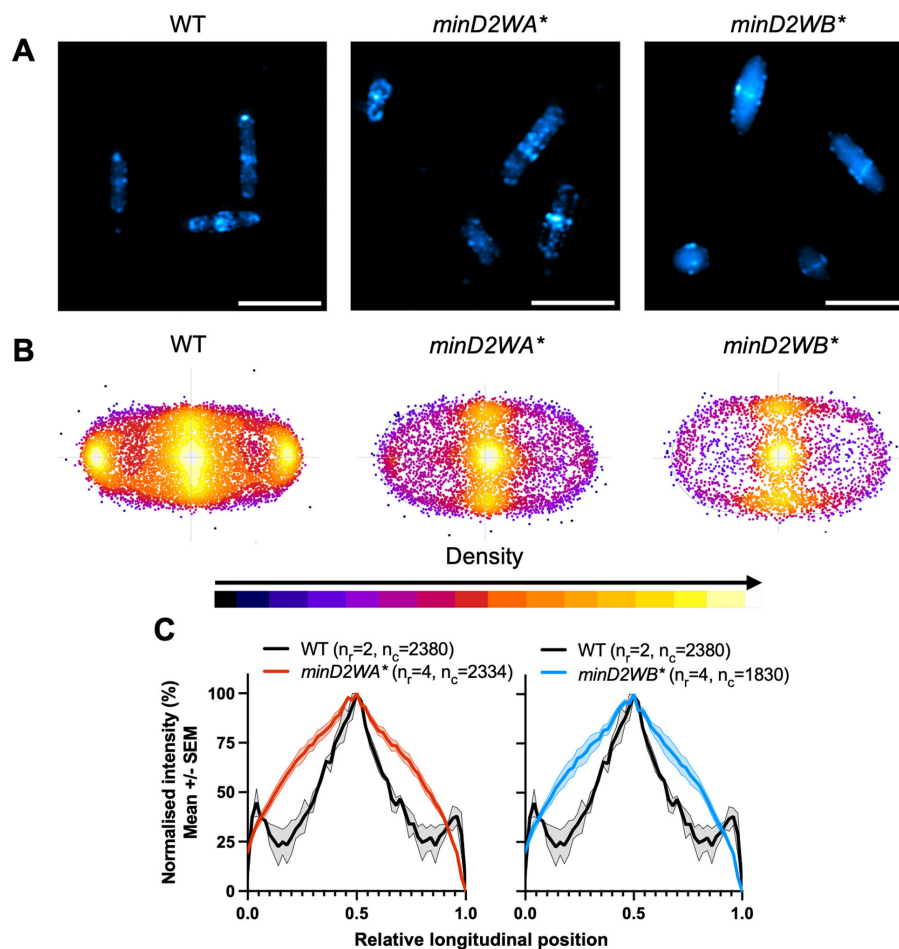


FIGURE 5

Chromosomal Walker mutants of *minD2* disrupt polar localization of CetZ1. H26 wildtype and *minD2* walker mutant strains containing pHVID135 (for expression of CetZ1-mTq2) were grown in Hv-Cab with 1 mM L-Tryptophan and sampled at  $OD_{600} \sim 0.1$ . (A) Cells were imaged using epifluorescence to observe CetZ1-mTq2 localization. Scale bar 5  $\mu$ m. (B) Heat map representations of detected foci of CetZ1-mTq2 and their localisations. Heatmaps are colored by density, referring to subcellular localization along the relative length of lateral and longitudinal axes only and do not fluorescence intensity. (C) Normalized median fluorescence intensity of CetZ1-mTq2 along the long axis of the cell, represented as the mean (bold line) and standard deviation (shading) of biological replicates (as in Figure 2D). Two biological replicates were carried out for the wildtype background, and four for each of *minD2WA\** and *minD2WB\**, and data for H26 wildtype is included on both graphs for reference. The number of culture replicates ( $n_r$ ) and number of cells ( $n_c$ ) measured from pooled replicates are indicated in the key of panel (C).

summarize several possibilities for the role of MinD proteins in motility and CetZ1 localization (Figure 6). In this model, MinD2 and MinD4 help direct the archaeellum (Arl) and chemotaxis (Che) proteins to the cell poles directly or via positioning and assembly of polar CetZ1. We recently found that CetZ1 plays a role in the proper placement of the motility machinery (Brown et al., 2024). However, the present finding that the chromosomal *minD2WA\** mutation blocked polar CetZ1 localization but only weakly affected motility suggests that MinD proteins might separately control both the position of CetZ1 and another aspect of motility, such as placement of the motility machinery at the cell poles, independently of MinD2 regulated CetZ1 positioning.

Previous work showed that MinD4 forms dynamic cell cap-like structures in an ATPase-dependent manner, and yet oscillates in the cells independently of ATPase function (Figure 6), suggesting that it interacts with another oscillator that drives the movement

(Nußbaum et al., 2020). The localization patterns of MinD2 are currently unknown due to the absence of functional fluorescently tagged MinD2 (Patro et al., 2024). However, our observations that the complex patterns of CetZ1 localization are affected by MinD2 at multiple sites and at a cellular scale would suggest that similar cellular level MinD2 pattern formation might exist.

In summary, our findings have showed that multiple MinD homologs can have differing functions and regulate the subcellular positioning of the archaeal tubulin-like protein CetZ1 in the context of the development of swimming motility. They represent the first demonstration of MinD proteins controlling the position of tubulin superfamily proteins in archaea. The MinD-controlled positioning of CetZ1 in distinct subcellular locations is consistent with multiple functions of CetZ1, evoking parallels with the multiple functions of tubulins and other eukaryotic cytoskeletal proteins that are extensively regulated in time and space.

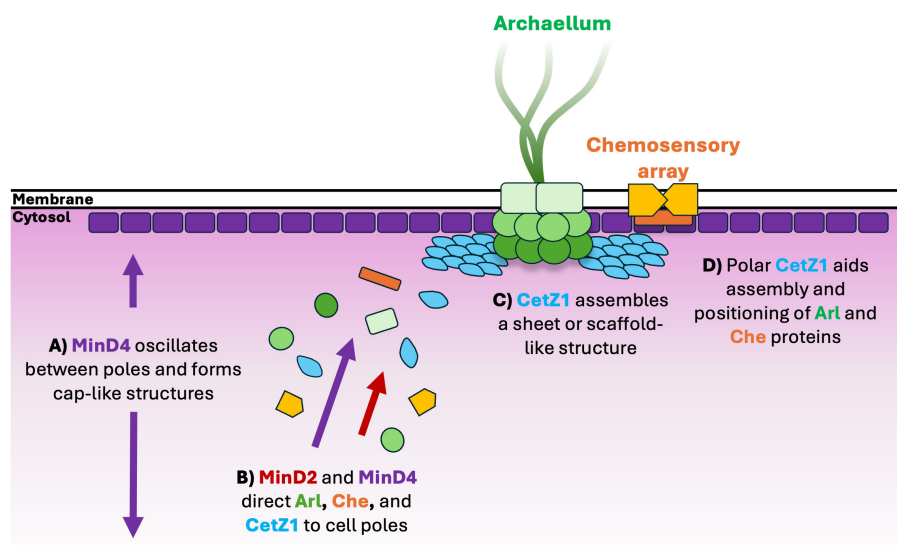


FIGURE 6

Schematic model for assembly of motility proteins at cell poles. (A) MinD4 oscillates between cell poles and forms cap-like localisations at cell poles in an ATPase dependent manner (Nußbaum et al., 2020). (B) MinD4 (Nußbaum et al., 2020) and MinD2 direct protein constituents of the archaeellum ("Arl") and chemosensory arrays ("Che") such as ArlD and CheW, respectively, to cell poles (Patro et al., 2024). CetZ1 is also directed to cell poles, likely by both MinD paralogs, but more dominantly by MinD2. (C) At cell poles, CetZ1 is hypothesized to assemble as a sheet or disc-like structure, (D) where it may contribute to assembly and positioning of motility structures via an unknown mechanism (Brown et al., 2024).

## Data availability statement

The original contributions presented in the study are included in the article/Supplementary material, further inquiries can be directed to the corresponding author.

## Author contributions

HB: Conceptualization, Data curation, Formal analysis, Investigation, Methodology, Validation, Visualization, Writing – original draft, Writing – review & editing. ID: Conceptualization, Funding acquisition, Methodology, Project administration, Supervision, Validation, Writing – review & editing.

## Funding

The author(s) declare financial support was received for the research, authorship, and/or publication of this article. The work was supported by the Australian Research Council (DP160101076 and FT160100010 to ID).

## Acknowledgments

The authors would like to acknowledge facilities support from L. Cole and A. Bottomley and the UTS Microbial Imaging Facility.

## Conflict of interest

The authors declare that the research was conducted in the absence of any commercial or financial relationships that could be construed as a potential conflict of interest.

The author(s) declared that they were an editorial board member of Frontiers, at the time of submission. This had no impact on the peer review process and the final decision.

## Publisher's note

All claims expressed in this article are solely those of the authors and do not necessarily represent those of their affiliated organizations, or those of the publisher, the editors and the reviewers. Any product that may be evaluated in this article, or claim that may be made by its manufacturer, is not guaranteed or endorsed by the publisher.

## Supplementary material

The Supplementary Material for this article can be found online at: <https://www.frontiersin.org/articles/10.3389/fmicb.2024.1474697/full#supplementary-material>

## References

- Abdul Halim, M. F., Pfeiffer, F., Zou, J., Frisch, A., Haft, D., Wu, S., et al. (2013). *Haloferax volcanii* archaeosortase is required for motility, mating, and C-terminal processing of the S-layer glycoprotein. *Mol. Microbiol.* 88, 1164–1175. doi: 10.1111/mmi.12248
- Abdul Halim, M. F., Schulze, S., DiLucido, A., Pfeiffer, F., Bisson Filho, A. W., Pohlschroder, M., et al. (2020). Lipid anchoring of archaeosortase substrates and midcell growth in haloarchaea. *MBio* 11:e00349–20. doi: 10.1128/mBio.00349-20
- Allers, T., Barak, S., Liddell, S., Wardell, K., and Mevarech, M. (2010). Improved strains and plasmid vectors for conditional overexpression of His-tagged proteins in *Haloferax volcanii*. *Appl. Environ. Microbiol.* 76, 1759–1769. doi: 10.1128/AEM.02670-09
- Allers, T., Ngo, H.-P., Mevarech, M., and Lloyd, R. G. (2004). Development of additional selectable markers for the halophilic archaeon *Haloferax volcanii* based on the *leuB* and *trpA* genes. *Appl. Environ. Microbiol.* 70, 943–953. doi: 10.1128/AEM.70.2.943-953.2004
- Aylett, C. H., and Duggin, I. G. (2017). “The tubulin superfamily in archaea,” in *Prokaryotic Cytoskeletons*, eds. J. Löwe, and L. Amos (Cham: Springer), 393–417. doi: 10.1007/978-3-319-53047-5\_14
- Babski, J., Haas, K. A., Nather-Schindler, D., Pfeiffer, F., Forstner, K. U., Hammelmann, M., et al. (2016). Genome-wide identification of transcriptional start sites in the haloarchaeon *Haloferax volcanii* based on differential RNA-Seq (dRNA-Seq). *BMC Genomics* 17:629. doi: 10.1186/s12864-016-2920-y
- Baxter, J. C., and Funnell, B. E. (2015). “Plasmid partition mechanisms,” in *Plasmids: Biology and Impact in Biotechnology and Discovery*, eds. M. E. Tolmashy, and J. C. Alonso (Hoboken, NJ: Wiley), 133–155. doi: 10.1128/9781555818982.ch8
- Bi, E., Dai, K., Subbarao, S., Beall, B., and Lutkenhaus, J. (1991). FtsZ and cell division. *Res. Microbiol.* 142, 249–252. doi: 10.1016/0923-2508(91)90037-B
- Brown, H. J., and Duggin, I. G. (2023). Diversity and potential multifunctionality of archaeal CetZ Tubulin-like cytoskeletal proteins. *Biomolecules* 13:134. doi: 10.3390/biom13010134
- Brown, H. J., Islam, M. I., Ruan, J., Baker, M. A., Ithurbe, S., Duggin, I. G., et al. (2024). CetZ1-dependent polar assembly of the motility machinery in haloarchaea. *bioRxiv* 2024.05.02.592137. doi: 10.1101/2024.05.02.592137
- Cerletti, M., Gimenez, M. I., Da Troetschel, C., D’Alessandro, C., Poetsch, A., De Castro, R. E., et al. (2018). Proteomic study of the exponential-stationary growth phase transition in the Haloarchaea *Natrialba magadii* and *Haloferax volcanii*. *Proteomics* 18:e1800116. doi: 10.1002/pmic.201800116
- Cerletti, M., Martínez, M. J., Giménez, M. I., Sastre, D. E., Paggi, R. A., and De Castro, R. E. (2014). The LonB protease controls membrane lipids composition and is essential for viability in the extremophilic haloarchaeon *Haloferax volcanii*. *Environ. Microbiol.* 16, 1779–1792. doi: 10.1111/1462-2920.12385
- Chatterjee, P., Garcia, M., Cote, J., Yun, K., Legerme, G., Habib, R., et al. (2024). Involvement of ArII, ArI, and CirA in archaeal type-IV pilin-mediated motility regulation. *bioRxiv* 2024.03.04.583388. doi: 10.1101/2024.03.04.583388
- Cline, S. W., Lam, W. L., Charlebois, R. L., Schalkwyk, L. C., and Doolittle, W. F. (1989). Transformation methods for halophilic archaeobacteria. *Can. J. Microbiol.* 35, 148–152. doi: 10.1139/m89-022
- De Boer, P. A., Crossley, R. E., and Rothfield, L. I. (1989). A division inhibitor and a topological specificity factor coded for by the *minicell* locus determine proper placement of the division septum in *E. coli*. *Cell* 56, 641–649. doi: 10.1016/0092-8674(89)90586-2
- de Silva, R. T., Abdul-Halim, M. F., Pittrich, D. A., Brown, H. J., Pohlschroder, M., Duggin, I. G., et al. (2021). Improved growth and morphological plasticity of *Haloferax volcanii*. *Microbiology* 167:001012. doi: 10.1099/mic.0.001012
- de Silva, R. T., Shinde, V., Brown, H. J., Liao, Y., and Duggin, I. G. (2024). Dynamic self-association of archaeal tubulin-like protein CetZ1 drives *Haloferax volcanii* morphogenesis. *bioRxiv* 2024.04.08.588506. doi: 10.1101/2024.04.08.588506
- Ducret, A., Quardokus, E. M., and Brun, Y. V. (2016). MicrobeJ, a tool for high throughput bacterial cell detection and quantitative analysis. *Nat. Microbiol.* 1, 1–7. doi: 10.1038/nmicrobiol.2016.77
- Duggin, I. G., Aylett, C. H., Walsh, J. C., Michie, K. A., Wang, Q., Turnbull, L., et al. (2015). CetZ tubulin-like proteins control archaeal cell shape. *Nature* 519, 362. doi: 10.1038/nature13983
- Dunham, T. D., Xu, W., Funnell, B. E., and Schumacher, M. A. (2009). Structural basis for ADP-mediated transcriptional regulation by P1 and P7 ParAn. *EMBO J.* 28, 1792–1802. doi: 10.1038/emboj.2009.120
- Erickson, H. P. (1995). FtsZ, a prokaryotic homolog of tubulin? *Cell* 80, 367–370. doi: 10.1016/0092-8674(95)90486-7
- Esquivel, R. N., and Pohlschroder, M. (2014). A conserved type IV pilin signal peptide H-domain is critical for the post-translational regulation of flagella-dependent motility. *Mol. Microbiol.* 93, 494–504. doi: 10.1111/mmi.12673
- Hackley, R. K., Hwang, S., Herb, J. T., Bhanap, P., Lam, K., Vreugdenhil, A., et al. (2024). TbsP and TrmB jointly regulate gapII to influence cell development phenotypes in the archaeon *Haloferax volcanii*. *Mol. Microbiol.* 121, 742–766. doi: 10.1111/mmi.15225
- Howard, M., and Kruse, K. (2005). Cellular organization by self-organization: mechanisms and models for Min protein dynamics. *J. Cell Biol.* 168:533. doi: 10.1083/jcb.200411122
- Hu, Z., and Lutkenhaus, J. (2001). Topological regulation of cell division in *E. coli*: spatiotemporal oscillation of MinD requires stimulation of its ATPase by MinE and phospholipid. *Mol. Cell* 7, 1337–1343. doi: 10.1016/S1097-2765(01)00273-8
- Ithurbe, S., de Silva, R. T., Brown, H. J., Shinde, V., and Duggin, I. G. (2024). A vector system for single and tandem expression of cloned genes and multi-colour fluorescent tagging in *Haloferax volcanii*. *Microbiology* 170:001461. doi: 10.1099/mic.0.001461
- Jalal, A. S., and Le, T. B. (2020). Bacterial chromosome segregation by the ParABS system. *Open Biol.* 10:200097. doi: 10.1098/rsob.200097
- Laass, S., Monzon, V. A., Kliemt, J., Hammelmann, M., Pfeiffer, F., Forstner, K. U., et al. (2019). Characterization of the transcriptome of *Haloferax volcanii*, grown under four different conditions, with mixed RNA-Seq. *PLoS ONE* 14:e0215986. doi: 10.1371/journal.pone.0215986
- Lackner, L. L., Raskin, D. M., and De Boer, P. A. (2003). ATP-dependent interactions between *Escherichia coli* Min proteins and the phospholipid membrane *in vitro*. *J. Bacteriol.* 185, 735–749. doi: 10.1128/JB.185.3.735-749.2003
- Laloux, G., and Jacobs-Wagner, C. (2014). How do bacteria localize proteins to the cell pole? *J. Cell Sci.* 127, 11–19. doi: 10.1242/jcs.138628
- Leipe, D. D., Wolf, Y. I., Koonin, E. V., and Aravind, L. (2002). Classification and evolution of P-loop GTPases and related ATPases. *J. Mol. Biol.* 317, 41–72. doi: 10.1006/jmbi.2001.5378
- Li, Z., Kinoshita, Y., Rodriguez-Franco, M., Nussbaum, P., Braun, F., Delpach, F., et al. (2019). Positioning of the motility machinery in halophilic archaea. *MBio* 10:e00377-19. doi: 10.1128/mBio.00377-19
- Loose, M., Fischer-Friedrich, E., Herold, C., Kruse, K., and Schwill, P. (2011). Min protein patterns emerge from rapid rebinding and membrane interaction of MinE. *Nat. Struct. Mol. Biol.* 18, 577–583. doi: 10.1038/nsmb.2037
- Lutkenhaus, J. (2007). Assembly dynamics of the bacterial MinCDE system and spatial regulation of the Z ring. *Annu. Rev. Biochem.* 76, 539–562. doi: 10.1146/annurev.biochem.75.103004.142652
- Lutkenhaus, J. (2012). The ParA/MinD family puts things in their place. *Trends Microbiol.* 20, 411–418. doi: 10.1016/j.tim.2012.05.002
- Lutkenhaus, J., and Sundaramoorthy, M. (2003). MinD and role of the deviant Walker A motif, dimerization and membrane binding in oscillation. *Mol. Microbiol.* 48, 295–303. doi: 10.1046/j.1365-2958.2003.03427.x
- Nogales, E., Downing, K. H., Amos, L. A., and Löwe, J. (1998). Tubulin and FtsZ form a distinct family of GTPases. *Nat. Struct. Mol. Biol.* 5:451. doi: 10.1038/nsb0698-451
- Nussbaum, P., Ithurbe, S., Walsh, J. C., Patro, M., Delpach, F., Rodriguez-Franco, M., et al. (2020). An oscillating MinD protein determines the cellular positioning of the motility machinery in archaea. *Cur. Biol.* 30, 4956–4972. e4. doi: 10.1016/j.cub.2020.09.073
- Park, K.-T., Wu, W., Battaile, K. P., Lovell, S., Holyoak, T., Lutkenhaus, J., et al. (2011). The Min oscillator uses MinD-dependent conformational changes in MinE to spatially regulate cytokinesis. *Cell* 146, 396–407. doi: 10.1016/j.cell.2011.06.042
- Patro, M., Duggin, I. G., Albers, S. V., and Ithurbe, S. (2023). Influence of plasmids, selection markers and auxotrophic mutations on *Haloferax volcanii* cell shape plasticity. *Front. Microbiol.* 14:1270665. doi: 10.3389/fmicb.2023.1270665
- Patro, M., Sivabalasarma, S., Gfrerer, S., Rodriguez-Franco, M., Nussbaum, P., Ithurbe, S., et al. (2024). MinD2 modulates cell shape and motility in the archaeon *Haloferax volcanii*. *bioRxiv* 2024.08.01.606218. doi: 10.1101/2024.08.01.606218
- Perez-Cheeks, B. A., Planet, P. J., Sarkar, I. N., Clock, S. A., Xu, Q., and Figurski, D. H. (2012). The product of *tadZ*, a new member of the parA/minD superfamily, localizes to a pole in *Aggregatibacter actinomycetemcomitans*. *Mol. Microbiol.* 83, 694–711. doi: 10.1111/j.1365-2958.2011.07955.x
- Raskin, D. M., and De Boer, P. A. (1999). Rapid pole-to-pole oscillation of a protein required for directing division to the middle of *Escherichia coli*. *Proc. Nat. Acad. Sci.* 96, 4971–4976. doi: 10.1073/pnas.96.9.4971
- Ringgaard, S., Schirner, K., Davis, B. M., and Waldor, M. K. (2011). A family of ParA-like ATPases promotes cell pole maturation by facilitating polar localization of chemotaxis proteins. *Genes Dev.* 25, 1544–1555. doi: 10.1101/gad.2061811

- Roberts, M. A., Wadhams, G. H., Hadfield, K. A., Tickner, S., and Armitage, J. P. (2012). ParA-like protein uses nonspecific chromosomal DNA binding to partition protein complexes. *Proc. Natl. Acad. Sci.* 109, 6698–6703. doi: 10.1073/pnas.1114000109
- Savage, D. F., Afonso, B., Chen, A. H., and Silver, P. A. (2010). Spatially ordered dynamics of the bacterial carbon fixation machinery. *Science* 327, 1258–1261. doi: 10.1126/science.1186090
- Schiller, H., Hong, Y., Kouassi, J., Rados, T., Kwak, J., DiLucido, A., et al. (2024). Identification of structural and regulatory cell-shape determinants in *Haloferax volcanii*. *Nat. Commun.* 15:1414. doi: 10.1038/s41467-024-45196-0
- Schindelin, J., Arganda-Carreras, I., Frise, E., Kaynig, V., Longair, M., Pietzsch, T., et al. (2012). Fiji: an open-source platform for biological-image analysis. *Nat. Methods* 9:676. doi: 10.1038/nmeth.2019
- Schmid, B., Tripal, P., Fraaß, T., Kersten, C., Ruder, B., Grüneboom, A., et al. (2019). 3Dscript: animating 3D/4D microscopy data using a natural-language-based syntax. *Nat. Methods* 16, 278–280. doi: 10.1038/s41592-019-0359-1
- Schuhmacher, J. S., Rossmann, F., Dempwolff, F., Knauer, C., Altegoer, F., Steinchen, W., et al. (2015b). MinD-like ATPase FlhG effects location and number of bacterial flagella during C-ring assembly. *Proc. Nat. Acad. Sci.* 112, 3092–3097. doi: 10.1073/pnas.1419388112
- Schuhmacher, J. S., Thormann, K. M., and Bange, G. (2015a). How bacteria maintain location and number of flagella? *FEMS Microbiol. Rev.* 39, 812–822. doi: 10.1093/femsre/fuv034
- Szeto, T. H., Rowland, S. L., Rothfield, L. I., and King, G. F. (2002). Membrane localization of MinD is mediated by a C-terminal motif that is conserved across eubacteria, archaea, and chloroplasts. *Proc. Nat. Acad. Sci.* 99, 15693–15698. doi: 10.1073/pnas.232590599
- Thompson, S. R., Wadhams, G. H., and Armitage, J. P. (2006). The positioning of cytoplasmic protein clusters in bacteria. *Proc. Nat. Acad. Sci.* 103, 8209–8214. doi: 10.1073/pnas.0600919103
- Tripepi, M., Imam, S., and Pohlschröder, M. (2010). *Haloferax volcanii* flagella are required for motility but are not involved in PibD-dependent surface adhesion. *J. Bacteriol.* 192, 3093–3102. doi: 10.1128/JB.00133-10
- Tripepi, M., You, J., Temel, S., Önder, Ö., Brisson, D., Pohlschröder, M., et al. (2012). N-glycosylation of *Haloferax volcanii* flagellins requires known Agl proteins and is essential for biosynthesis of stable flagella. *J. Bacteriol.* 194, 4876–4887. doi: 10.1128/JB.00731-12
- Zhou, H., Schulze, R., Cox, S., Saez, C., Hu, Z., Lutkenhaus, J., et al. (2005). Analysis of MinD mutations reveals residues required for MinE stimulation of the MinD ATPase and residues required for MinC interaction. *J. Bacteriol.* 187, 629–638. doi: 10.1128/JB.187.2.629-638.2005